

Review

Recent Advances in Aluminum Welding for Marine Structures

Bai-Qiao Chen ^{1,2,*} , Kun Liu ¹ and Sheng Xu ¹

¹ School of Naval Architecture and Ocean Engineering, Jiangsu University of Science and Technology, Zhenjiang 212003, China

² Centre for Marine Technology and Ocean Engineering (CENTEC), Instituto Superior Técnico, Universidade de Lisboa, 1049-001 Lisbon, Portugal

* Correspondence: baiqiao.chen@tecnico.ulisboa.pt

Abstract: This review explores the recent advancements in welding techniques for aluminum plates utilized in ships and offshore structures, with a particular focus on minimizing weld-induced deformation and residual stress to improve structural performance. Given the critical role of welding in the construction and repair of marine structures, understanding the influence of these factors is paramount. This article synthesizes current research findings, evaluates the effectiveness of various welding methods, and highlights innovative approaches to reduce adverse effects. Through a comprehensive analysis of experimental and simulation studies, this review identifies key strategies for optimizing welding processes, thereby contributing to the durability and integrity of marine structures. This synthesis not only highlights successful strategies for optimizing welding processes but also offers guidance for researchers and practitioners in the field. This review also identifies previously unaddressed gaps in the literature, particularly focusing on the underexplored interactions between specific welding parameters and the long-term durability of marine structures, offering new perspectives and directions for future research. It delineates critical challenges faced in the welding of aluminum alloys for marine applications and offers targeted suggestions to address these issues, thereby paving the way for advancements in welding practices and technology. The findings aim to guide researchers and industry practitioners in selecting and developing welding techniques that ensure the safety, reliability, and longevity of marine infrastructure.

Keywords: welding; residual stress; aluminum; shipbuilding; offshore structure; ultimate strength; digital twin; finite element analysis



Citation: Chen, B.-Q.; Liu, K.; Xu, S. Recent Advances in Aluminum Welding for Marine Structures. *J. Mar. Sci. Eng.* **2024**, *12*, 1539. <https://doi.org/10.3390/jmse12091539>

Academic Editor: Pasqualino Corigliano

Received: 12 August 2024
Revised: 25 August 2024
Accepted: 25 August 2024
Published: 4 September 2024



Copyright: © 2024 by the authors. Licensee MDPI, Basel, Switzerland. This article is an open access article distributed under the terms and conditions of the Creative Commons Attribution (CC BY) license (<https://creativecommons.org/licenses/by/4.0/>).

1. Introduction

The utilization of aluminum alloys in the construction of marine structures, such as ships and offshore platforms, is driven by their favorable properties: lightweight, high strength-to-weight ratio, and exceptional corrosion resistance. These characteristics are particularly advantageous in reducing the overall mass of structures, which can lead to significant improvements in operational efficiency and durability [1–3]. Driven by the need for structural weight reduction and the operation of aluminum vessels and offshore structures in more challenging seaway conditions, there has been a growing interest in applying limit-state design and analysis procedures. These methods necessitate assessing the ultimate strength of aluminum structural members [4,5].

The manufacturing of seagoing vessels from aluminum commenced post-World War II, coinciding with advancements in fusion welding technology and the development of the 5xxx series of aluminum alloys (commonly referred to as Al–Mg alloys) [6,7]. While large merchant ships are typically constructed from steel, naval vessels, especially small to moderate-sized merchant ships and high-speed patrol vessels, are increasingly utilizing marine-grade aluminum alloys where reducing weight is crucial [8].

Aluminum is also extensively used in offshore platforms due to its corrosion resistance, strength-to-weight ratio, and ease of fabrication [7,9]. It finds applications in superstruc-

tures, living quarters, safety features like handrails and walkways, and critical systems such as heat exchangers and cooling systems. It is the material of choice for building helidecks and helipads, which benefit from its light weight and durability against harsh marine conditions. Additionally, living quarters and other accommodation modules on offshore platforms often feature aluminum to ensure structural integrity and resistance to environmental wear. Lift boats and temporary work platforms also capitalize on aluminum's light weight, enhancing their mobility and ease of repositioning. For masts and communication towers, aluminum's robustness and anticorrosive properties make it ideal, ensuring long-term reliability. Moreover, in fire control systems, aluminum is favored for its fire resistance and lightness, which are critical for safety components like panels and doors. Its noncombustible properties enhance fire safety measures on platforms, showcasing its versatility in marine engineering [10].

Standards for aluminum ships and offshore structures are crucial for ensuring safety, durability, and performance. These standards cover various aspects such as material properties, design criteria, fabrication processes, and testing methodologies. The International Association of Classification Societies (IACS), Det Norske Veritas (DNV), Lloyd's Register (LR), and Eurocode 9 offer classification options for ultimate hull-girder strength assessment [11–14].

Recent advancements in welding technology have further enhanced the viability of aluminum in marine applications [6,8,15]. Metal inert gas (MIG) welding, initially developed in the 1940s for welding aluminum and other nonferrous materials, remains the most prevalent industrial welding process today [16–18]. Nevertheless, innovative welding methods such as friction stir welding (FSW) [19–23] and laser beam welding (LBW) [24–26] have shown promising results in minimizing deformation and improving the overall quality of the joints in aluminum structures.

However, the welding of aluminum plates is not without challenges, primarily due to the material's susceptibility to weld-induced deformation and residual stresses. These phenomena can severely compromise the structural integrity and longevity of marine structures, making the study of advanced welding techniques a critical area of research [27–31]. A thorough sensitivity analysis grounded on a benchmark provided by the International Ship and Offshore Structures Congress (ISSC) has demonstrated that the ultimate strength of aluminum structures is significantly affected not only by the yield stress and the degradation of mechanical strength in heat-affected zones (HAZs) but also by weld-induced residual stresses (WRSs) and geometric imperfections [32].

Additionally, hot cracking and hydrogen-induced porosity are major challenges in aluminum welding [7,21,23]. Hot cracking occurs due to aluminum's susceptibility to thermal stresses during solidification, requiring careful assessment through mechanical tests and microscopic examination. Hydrogen-induced porosity, caused by the high solubility of hydrogen in molten aluminum, compromises weld integrity. Addressing these issues involves meticulous pre-weld cleaning, the use of inert gas shielding, and strategic post-weld treatments to enhance the structural reliability of welded joints.

Welding aluminum alloys requires a higher skill level than welding other materials due to its quick reaction to heat and propensity for forming defects [33,34]. Aluminum has a high thermal conductivity, which means that it dissipates heat quickly. This characteristic can lead to uneven heat distribution during the welding process, making it difficult to achieve consistent weld penetration, and this can increase the likelihood of weld defects. The conventional welding techniques need to be adjusted or modified when applied to aluminum alloys. For instance, aluminum's high thermal conductivity requires higher power settings or faster welding speeds than those used for steel to achieve similar penetration [25,35–38].

Compared to laboratory experiments (e.g., [39–43]), the finite element method (FEM) offers a more cost-effective and quicker alternative for analyzing the welding process. The main FEM approaches used in welding simulations include the thermo–elasto–plastic (TEP) method [28,44–46], the elastic method [30], and the inherent strain method [47–49]. More

recently, Chen et al. [50–52] have developed models and techniques to predict distortions and residual stresses induced in ship plates by welding. Additionally, the impacts of the convection coefficient, finite element meshes, sequences, and boundary conditions have also been explored [17,18,53,54]. On the other hand, highly detailed FEM simulations, especially those involving complex weld geometries and sophisticated material behavior models, can be computationally intensive. They require significant computational resources and time, which can be a limiting factor in some applications.

This review aims to synthesize recent findings from the field, providing a comprehensive overview of current technologies and methodologies in welding aluminum for marine use, with a particular emphasis on identifying and analyzing the most significant challenges in this field. The objectives of the research include the following: (1) reviewing the latest developments in welding techniques suited for aluminum in marine settings; (2) assessing the effectiveness of these techniques in overcoming common welding challenges; (3) exploring the impact of welding parameters on the structural integrity of marine aluminum structures; and (4) proposing practical recommendations and future research directions based on identified gaps in current knowledge. By highlighting the latest developments and their implications for structural performance, this article seeks to contribute valuable insights to both academic researchers and industry practitioners.

2. Literature Review Methodology

This review was systematically conducted to ensure a comprehensive analysis of recent developments in aluminum welding for marine applications. The methodology employed involved a structured literature search focusing on peer-reviewed journals, conference proceedings, and authoritative industry reports and guidelines published within the last decade. For this review, the Web of Science Core Collection database served as the primary source for conducting a comprehensive literature search. It provided access to a wide range of peer-reviewed articles, ensuring that the studies selected for review were relevant and of high scholarly standards.

The selection criteria were based on relevance to aluminum welding technologies, application to marine environments, and contributions to advancements in welding processes or understanding of welding phenomena. Over 20,000 articles were identified on the topic of aluminum welding, reflecting the broad and extensive research in this area. To refine this vast pool of literature, articles were initially filtered by abstracts that matched our specific research queries on welding techniques, heat effects, material properties, and application-specific challenges. This filtering process significantly narrowed the scope, resulting in a much more manageable subset of articles. Subsequently, full texts were reviewed to ensure they provided significant insights into the current trends, challenges, and innovations in the field.

To maintain the integrity of our review, only studies that met these criteria and offered empirical data or theoretical analysis relevant to marine applications of aluminum welding were included, culminating in the selection of 118 papers that form the core of this literature review. This methodological rigor ensures that our conclusions are drawn from a broad and relevant set of sources, providing a holistic view of the state of the art in the field.

The literature review for this manuscript primarily focuses on the most recent developments in aluminum welding for marine applications, with a significant emphasis on publications from the last four years. Specifically, the review includes 51 references from 2020 to 2024, demonstrating a strong orientation towards cutting-edge research and the latest advancements in the field. In addition to this recent literature, we have also incorporated three classic papers from the 1980s and 1990s, which are seminal works providing foundational insights that continue to influence current practices and theories. This combination ensures that the review captures both the most up-to-date technologies and the historical underpinnings of key methodologies, offering a comprehensive and relevant overview of the subject.

3. Fundamentals of Welding Aluminum for Marine Applications

3.1. Aluminum Alloys in Marine Construction

Aluminum alloys are increasingly utilized in marine applications due to their excellent strength-to-weight ratio, corrosion resistance, and weldability. The specific aluminum alloy series commonly employed include the 5xxx and 6xxx series, which are prized for their superior durability in marine environments. These alloys not only withstand the corrosive sea water but also offer significant weight savings over traditional shipbuilding materials like steel. This reduction in weight translates to higher fuel efficiency and lower operating costs, making aluminum alloys a favorable choice for modern marine construction projects. The chemical compositions of aluminum alloys that comply with the IACS rules are listed in Table 1, where the values are in percentage mass by mass maximum unless shown as a range or as a minimum.

Table 1. Chemical composition of aluminum alloys for marine structures by IACS requirement. Reconstructed table with data from [11].

Grade	Si	Fe	Cu	Mn	Mg	Cr	Zn	Ti	Others
5059	0.45	0.50	0.25	0.60–1.2	5.0–6.0	0.25	0.4–0.9	0.20	0.15
5083	0.40	0.40	0.10	0.41–1.0	4.0–4.9	0.05–0.25	0.25	0.15	0.15
5086	0.40	0.50	0.10	0.20–0.7	3.5–4.5	0.05–0.25	0.25	0.15	0.15
5383	0.25	0.25	0.20	0.70–1.0	4.0–5.2	0.25	0.40	0.15	0.15
5456	0.25	0.40	0.10	0.50–1.0	4.7–5.5	0.05–0.20	0.25	0.20	0.15
5754	0.40	0.40	0.10	0.50	2.6–3.6	0.30	0.20	0.15	0.15
6005A	0.5–0.9	0.35	0.30	0.50	0.4–0.7	0.30	0.20	0.10	0.15
6061	0.4–0.8	0.7	0.15–0.4	0.15	0.8–1.2	0.04–0.35	0.25	0.15	0.15
6082	0.7–1.3	0.50	0.10	0.40–1.0	0.6–1.2	0.25	0.20	0.10	0.15

Some of the frequent alloying elements for aluminum include silicon, magnesium, manganese, chromium, and copper, among others. Silicon (Si) is often added to aluminum alloys to improve weldability by reducing the alloy’s melting temperature, which facilitates easier formation of the weld pool. It is fairly inexpensive and also helps to reduce hot cracking, a common issue in aluminum welding. Copper (Cu) can increase strength but adversely affects weldability by making the alloy more prone to cracking. Alloys with higher copper content typically require more careful welding techniques to manage these effects. Both manganese (Mn) and chromium (Cr) act as stabilizers in aluminum alloys, improving weldability by controlling grain structure during welding. Magnesium (Mg) enhances the strength of the alloy but can reduce weldability if present in high amounts due to increased cracking susceptibility. However, when balanced with silicon (as in the 6xxx series), magnesium can enhance weld strength without significantly compromising weldability.

In the four-digit number system of aluminum alloys (e.g., 5083, 6082), the first digit indicates the principal or major constituent alloy to describe the series, whereas the second single digit indicates the modification made in the original alloy. The last two digits are arbitrary numbers used to identify the specific alloy in the series. In this way, the material properties can vary offering various options for different applications. For example, for the numbers in the alloy 5383, the number 5 shows that it is of the magnesium alloy series, the 3 means the third modification to the original alloy 5083, and 83 identifies it in the 5xxx series.

Research focusing on the structural response of aluminum alloys has primarily concentrated on the 5xxx and 6xxx series. These alloys are particularly favored for structural engineering applications due to their superior mechanical properties. The 5xxx series, known for its excellent corrosion resistance, is ideal for structural components that are frequently exposed to harsh marine conditions. This series provides not only resilience against corrosion but also maintains substantial strength, which is crucial for the structural integrity of marine vessels. These characteristics are particularly important in applications

where long-term durability and minimal maintenance are critical, such as in hulls and deckhouse structures.

The 6xxx series is noted for its combination of strength and formability, allowing for more complex designs without compromising the structural integrity. This series adapts well to various fabrication processes, including intricate welding techniques required for the complex geometries of modern marine architecture. It is particularly favored for components like superstructures and framing where higher strength is necessary. Notably versatile, the 6xxx series alloys are easily extrudable, allowing them to be formed into complex shapes such as bulb, T-, and L-sections, along with closed-section stiffeners like trapezoidal stiffeners. Commonly, these alloys are employed in constructing deck panels and marine frames for ships [7].

Considering the ongoing challenges with mobility and congestion in the European transport industry, it may be beneficial to explore the construction of new aluminum vessels, such as catamarans and tourist ships. Aluminum profiles are essential in the design of fast catamarans due to their lightweight and strong characteristics, which contribute to increased speed and improved fuel efficiency. Notable examples include Austal's Benchi-jigua Express [55], a 127-meter trimaran fast ferry operating in the Canary Islands, and the 112-meter-long Natchan World, built by Incat, which serves routes in Japan [56]. In Portugal, Italy, and some other European countries, catamarans have been operating on the rivers since 2004 [57].

It should be noted that there is a scarcity of literature specifically dedicated to the global aspects of marine structures in the context of aluminum welding, as the majority of the studies referenced are centered around the behavior of local structural members, plates, and stiffened panels, which are fundamental structural components of ships and offshore structures.

3.2. *Welding Techniques for Aluminum in Marine Construction*

Several welding techniques are commonly employed for joining aluminum in marine construction, each with its advantages and applications.

3.2.1. GMAW/MIG

Gas metal arc welding (GMAW), also known as MIG welding, is popular for its versatility and the high quality of welds it produces [8,41,58–60]. It employs consumable wire electrodes that melt in an electric arc between the cut and the tip. The arc and weld pool are shielded by a protective gas emitted from nozzles. Originally developed in the 1940s for welding aluminum and other nonferrous materials, the MIG welding remains the most prevalent industrial welding process today, despite the advent of innovative techniques [61]. However, it requires careful control of welding parameters to avoid common issues like spatter and burn-through.

Most marine structural components, such as decks and bulkheads, can be constructed using the GMAW process [1,6,7,40,41]. For instance, an experiment using the GMAW process on a rectangular plate made of 5052-H32 aluminum alloy was detailed in [39]. Aluminum alloy 4043 filler wires with a diameter of 1.59 mm were utilized, with the welding parameters set to a current of 260 A and an arc voltage of 23 V. The plate dimensions were 1220 mm in length, 152.4 mm in width, and 12.5 mm in thickness. The welding torch moved along the longitudinal upper edge of the plate at a constant speed of 7.34 mm/s.

3.2.2. CMT & AM

Recently, the cold metal transfer (CMT) welding process [61,62], often referred to as the short arc process, has been identified as a variant of GMAW that utilizes different heat input ratios.

In addition, additive manufacturing (AM) is revolutionizing the repair and fabrication of aluminum structures [15]. This technology enables precise deposition of material, layer by layer, to build or repair parts directly from digital models.

3.2.3. GTAW/TIG

GTAW or tungsten inert gas (TIG) welding is preferred for its ability to produce high-quality, precise welds on thinner materials [59,61]. It uses a wire filler that is outside the welding arc. Though slower and more labor-intensive than GMAW, GTAW is excellent for applications requiring high aesthetic quality and minimal post-weld machining. In [34], GTAW was applied to test Al5083-H111 alloy plates with dimensions of $15 \times 300 \times 180 \text{ mm}^3$. The study considered heat inputs up to 5 kJ/mm and torch speeds ranging from 1 to 4 mm/s.

3.2.4. FSW

Friction stir welding (FSW) is a relatively newer technology that offers excellent control over weld distortion and residual stresses [19–23,42–44], and it has been a game-changer for the shipbuilding and marine industries.

A rotating tool with a slightly shorter probe than the plate thickness is pressed against two adjoining plates, as illustrated in Figure 1. The probe generates frictional heat primarily from the high normal pressure and shearing action at the shoulder, softening the material around it. As the tool moves along the joint, the material is moved around the probe from the retreating side, where rotational motion counters forward motion, to the surrounding solid material. This extruded material solidifies to form a joint behind the tool.

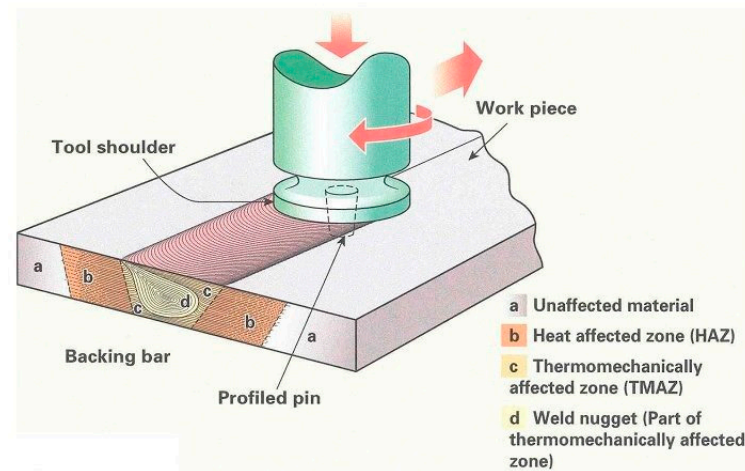


Figure 1. A visual representation of the FSW process detailing the critical zones and the interaction between the tool and the workpiece during welding. Source: <https://www.twi-global.com/technical-knowledge/job-knowledge/friction-stir-welding-147> (accessed on 24 August 2024).

Developed in 1991, this solid-state process is particularly useful for joining thicker aluminum plates commonly used in structural applications in ships and offshore platforms. More specifically, FSW is employed across various marine applications such as shipbuilding, underwater repairs, manufacturing of submersibles and propellers, offshore structures, retrofitting, and other marine components [43]. It also plays a vital role in the underwater maintenance and repair of offshore infrastructure like pipelines and oil rigs.

Additionally, FSW helps mitigate corrosion-related damage and maintains structural integrity in challenging aquatic environments. A study focusing on the application of FSW for joining aluminum 5451 components in marine structural applications was discussed in [42]. The dimensions of the AA5451 plate used were $900 \text{ mm} \times 60 \text{ mm} \times 6 \text{ mm}$. The study explored tool rotation speeds ranging from 1000 to 1400 rpm, feed rates from 16 to 20 mm/min, and three different tool pin profiles.

3.2.5. Laser Welding

Laser beam welding (LBW) is a precise, high-speed welding technique that uses a laser beam to create a concentrated heat source, allowing for deep penetration and minimal heat input [24–26,35–37]. This method is particularly beneficial for aluminum

alloys as it minimizes thermal distortion and allows for strong, high-quality welds in thin or thick sections.

Laser hybrid welding (LHW) combines the laser welding process with another welding process, usually arc welding (like MIG or TIG), to take advantage of both methods [25]. This synergy enhances weld quality by improving the consistency of the weld bead, increasing penetration depth, and reducing porosity and cracking tendencies in aluminum alloys. This technique is especially useful for joining thicker aluminum sections where single-method welding might struggle with penetration and weld integrity.

3.2.6. Summary

The most appropriate welding method needs to be selected based on specific project requirements and constraints encountered in marine environments. Table 2 summarizes the advantages and limitations of the aforementioned aluminum welding techniques commonly employed in marine construction. Each technique presents a unique set of benefits and challenges, influencing their suitability for different marine applications.

Table 2. A comparative analysis of the advantages and limitations of various techniques used in aluminum welding.

Welding Technique	Advantages	Limitations
MIG	Fast, cost-effective, good for thick sections, adaptable to automated systems	Potential for porosity, requires skilled operators
TIG	High quality, precise welds, low distortion	Slower, costly, requires a high skill level
AM	Allows complex geometries, customizable material properties	High cost, requires specialized equipment and expertise
FSW	Excellent mechanical properties, no filler needed	Limited to certain geometries, high equipment cost
LBW	High depth-to-width ratio, minimal heat input	High initial cost, limited to thin materials

3.3. Challenges in Welding Aluminum

Welding aluminum presents unique challenges that differ significantly from welding steel. The high thermal conductivity of aluminum leads to faster heat dissipation, which can affect weld penetration and increase the likelihood of weld defects such as porosity and lack of fusion [6,63]. During the fabrication of aluminum alloys, porosity defects are more likely to occur due to contamination of the wire surface compared to other metallic materials, such as titanium and stainless steel [33]. Additionally, aluminum’s oxide layer, which forms naturally when aluminum is exposed to air, has a higher melting point than the underlying metal and can inhibit weld quality if not properly removed before welding [64]. Managing these challenges requires specific techniques and careful preparation to ensure strong, durable welds. Additionally, the formation of an HAZ during welding presents a complex problem, as its size, properties, and impact on the structural strength are still not precisely predictable [4,6,43].

The properties of aluminum can vary significantly with temperature [6,45,46,65]. Figure 2 shows an example of the temperature-dependent material properties, including the yield stress, Young’s modulus, thermal expansion coefficient, conductivity, specific heat, density, and convection coefficient, of aluminum alloy 6082-T6. As temperature rises, the yield stress of the material drops sharply, accompanied by relatively slower decreases in Young’s modulus. Conversely, the thermal conductivity of aluminum alloy increases with temperature, surpassing 200 W/m/K at 400 °C, which is approximately three to six times higher than that of shipbuilding steel. The specific heat also varies but at a relatively slow rate, approximately twice that of shipbuilding steel. It has also been noted that Young’s modulus of aluminum alloys is approximately one-third that of steel.

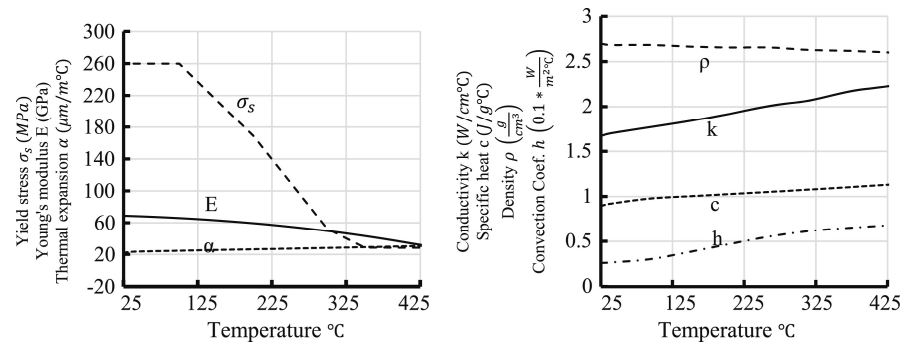


Figure 2. Material properties of aluminum alloy 6082-T6 that vary with temperature.

During welding, the HAZ in aluminum welds experiences a wide range of temperatures, leading to changes in material behavior such as melting, solidification, and thermally induced phase transformations. It is difficult to effectively model the HAZ to predict changes in microstructure and mechanical properties, due to the varying degrees of thermal exposure within the HAZ.

The stress–strain curve for aluminum alloys typically exhibits a more rounded profile compared to that of steel [66]. In theoretical and numerical analyses of aluminum structures, two primary types of material models are commonly used to assess ultimate strength: the actual stress–strain relationship derived from mechanical testing and approximate models such as the Ramberg–Osgood model. For accurate ultimate strength analyses of aluminum marine structures, it is crucial to consider the actual material behavior to achieve reliable results. In some studies [8,66], the Ramberg–Osgood approximation model is utilized as a substitute for the actual material behavior model. This approach differs from that used in steel structures, which are typically simulated using the elastic–perfectly plastic material model.

As the temperature increases, the yield strength of the aluminum alloy decreases, which can be described by the Arrhenius model [67]:

$$\sigma_y(T) = \sigma_0 \exp\left(-\frac{Q}{RT}\right) \tag{1}$$

where $\sigma_y(T)$ is the yield strength at temperature T , σ_0 is the yield strength at room temperature, Q is the thermal activation energy, R is the gas constant, and T is the absolute temperature. Additionally, the thermal expansion of aluminum alloys, affected by the product of the thermal expansion coefficient and the change in temperature, also influences the overall deformation during and after the welding process.

Furthermore, various defects such as porosity, inclusions, solidification cracking, and shrinkage can occur during the fusion welding of aluminum alloys, which diminish the aesthetics and mechanical properties of the welds [7]. Therefore, the marine sector needs innovative welding technologies to improve both the appearance and mechanical strength of welded structures.

3.4. Quality Control and Inspection Methods

The design of welds in aluminum structures must account for the material’s properties and the specific requirements of marine applications [11–14]. This includes selecting appropriate joint configurations and ensuring that the weld geometry helps distribute stresses evenly. Engineers must also consider the effects of thermal expansion and contraction in aluminum to minimize stress concentrations that could lead to cracking. The post-weld treatments [62,68,69] are crucial for restoring the strength and ductility affected by the welding heat. These may include heat treatments for stress relief and tempering to enhance the mechanical properties of the weld area.

Ensuring the quality of aluminum welds in marine constructions is critical for the safety and longevity of the structure. Nondestructive testing (NDT) methods such as ultrasonic testing [70,71], radiographic testing [72,73], and dye penetrant inspection (also called liquid penetrate inspection) [74,75] are routinely used to detect internal and surface defects. In addition, regular inspections are performed both during and after the construction process to ensure that all welding standards are met, and the structural integrity of the vessel or platform is maintained.

4. Simulation and Modeling of Welding Processes

FEM simulations of aluminum welding present a unique set of challenges due to the material's specific properties and the complexities of the welding process. Here are some of the main challenges faced when using FEM to model aluminum welds:

4.1. Complex Geometry of Weld Joints

Aluminum structures often feature complex joint geometries that are challenging to model accurately in FEM simulations. These geometries require refined meshing techniques to ensure that the finite element model can capture the nuances of the weld path and joint configuration. Figure 3 displays a finite element (FE) model of a plate welded using MIG, simulated in ANSYS Mechanical APDL, featuring hexahedral elements and regular connectivity, indicating a high-quality mesh and accurate solution outcomes. The dimensions of the butt-welded plate are $300 \times 150 \times 6 \text{ mm}^3$. Various element sizes (1.25, 2.5, 5, and 10 mm) are employed across different regions, including the fusion zone (FZ), HAZ, and the base material (BM). Transitional elements are employed to bridge areas with varying element sizes. Mesh refinement is specifically applied in the FZ and HAZ to enhance precision, while larger elements in the BM help reduce computational effort.

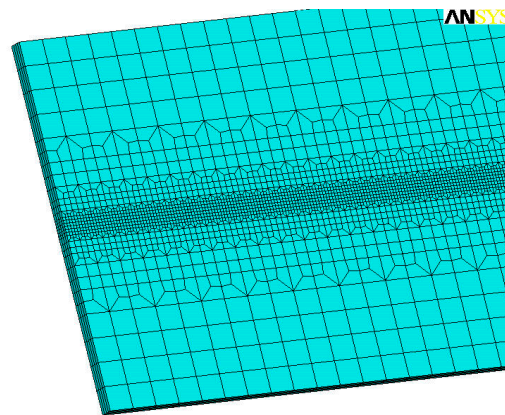


Figure 3. FE model of a welded plate with hexahedral elements.

4.2. Material Properties Variation

Aluminum has a high thermal conductivity compared to other metals like steel. This property leads to rapid heat dissipation during the welding process, which can affect the heat input requirements and the thermal gradients experienced during welding. The HAZ in aluminum welds is particularly susceptible to mechanical property deterioration due to the thermal cycle of the welding process. FEM needs to effectively model the HAZ to predict changes in microstructure and mechanical properties, which is difficult due to the varying degrees of thermal exposure within the HAZ.

Accurately modeling the transient material properties in FEM simulations is crucial but challenging, as it requires precise control and understanding of heat transfer mechanisms [6,76]. Despite extensive research, data on the temperature-dependent material properties of the BM are scarce, particularly at high temperatures. Traditionally, models have been developed based on room temperature property values and later validated.

A new simplified model was proposed in [6] to aid in the evaluation of weld-induced imperfections in structures composed of aluminum alloy 5052-H32:

$$k(T) = k_0 + 0.13T$$

$$\sigma_s(T) = \begin{cases} \sigma_{s0}, & 0 < T \leq 100 \text{ }^\circ\text{C} \\ \sigma_{s0} + 80 - 0.65T, & 100 < T < 380 \text{ }^\circ\text{C} \\ 0.08\sigma_{s0}, & T \geq 380 \text{ }^\circ\text{C} \end{cases} \quad (2)$$

where k is the thermal conductivity of the aluminum alloy, T represents the temperature, σ_s is the yield stress of the material, and the subscripted $_0$ means the value of the material property at room temperature.

In this model, thermal conductivity and yield stress are treated as temperature-dependent, using the proposed equations, while other material properties are considered constant at room temperature values. This simplified approach is particularly beneficial in welding simulations for aluminum alloys when high-temperature property data are not available.

4.3. Numerical Approaches

Due to aluminum’s lower yield strength and higher coefficient of thermal expansion, it is more prone to weld-induced distortions and residual stresses. Predicting the extent and distribution of these distortions and stresses using FEM is complicated and requires detailed models that can account for the complex interactions between thermal and mechanical fields.

Due to the significant impact of thermal processes on mechanical responses, an uncoupled thermal–mechanical formulation is commonly utilized to analyze the thermal–mechanical behavior during the welding process [17,18,28,40,41,48]. This approach considers the influence of the transient temperature field on stress via linear thermal expansion and incorporates temperature-dependent thermal physical and mechanical properties, as shown in Figure 4. In this type of finite element analysis (FEA), thermal and structural analyses are conducted independently and sequentially. The temperatures determined for all nodes in the initial thermal analysis stage are applied as body loads in the subsequent stage to the same geometric model to conduct the mechanical analysis.

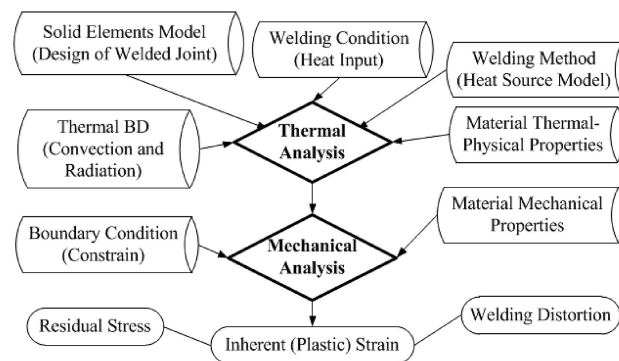


Figure 4. Flow chart of a transient nonlinear TEP-FEA. Adapted from [48], with permission from Elsevier (Amsterdam, The Netherlands), 2024.

During the heating and cooling phases of the welding process, the total strain can be categorized into various components, such as elastic strain, thermal strain, plastic strain, creep strain, and strain resulting from phase transformations. The concept of inherent strain encompasses the sum of thermal, plastic, creep, and phase transformation-induced strains. Essentially, inherent strain includes all forms of strain except for elastic strain, as expressed in the following equation:

$$\epsilon_{inherent} = \epsilon_{total} - \epsilon_{elastic} = \epsilon_{thermal} + \epsilon_{plastic} + \epsilon_{creep} + \epsilon_{phase} \quad (3)$$

Among all components of inherent strain, plastic strain is the predominant factor [28,30], which can be determined experimentally or assessed through TEP-FEAs. In the case of welded joints made from high-carbon steel, inherent strain is primarily represented by plastic strain, as the strain from creep and solid-state phase transformations is relatively minor [28]. Inherent strains are acknowledged as a key factor contributing to welding distortion. In practical terms, inherent deformation is categorized into two types: longitudinal inherent shrinkage force, known as tendon force, resulting from strong self-constraint, and transverse inherent shrinkage/bending, caused by weaker self-constraint [30]. Welding distortion is believed to arise from four specific components of inherent deformation: longitudinal shrinkage, transverse shrinkage, longitudinal bending, and transverse bending. These components of inherent deformation are described by the following equations [65]:

$$\begin{aligned} \delta_x &= \frac{1}{h} \iint \varepsilon_x^p dydz, \delta_y = \frac{1}{h} \iint \varepsilon_y^p dydz \\ \theta_x &= \frac{12}{h^3} \iint (z - h/2) \varepsilon_x^p dydz, \theta_y = \frac{12}{h^3} \iint (z - h/2) \varepsilon_y^p dydz \end{aligned} \tag{4}$$

where δ_x and δ_y are the longitudinal and transverse shrinkages, respectively; θ_x and θ_y are the longitudinal and transverse bendings, respectively; x , y , and z are the welding directions, transverse direction, and thickness direction, respectively; h is the thickness of the plate; ε_x^p and ε_y^p are the plastic strains obtained from the TEP-FEA.

The convection in the TEP-FEA is accounted for by utilizing the temperature-dependent values previously described in Section 3.3 [6,65]. For modeling radiation, the Stefan–Boltzmann law is employed, utilizing an emissivity value along with the Stefan–Boltzmann constant, which is approximately $5.67 \times 10^{-8} \text{ W/m}^2/\text{K}^4$ [26,45]. In addition to the TEP-FEM, elastic FEM that leverages inherent strain theory [28,30,47–49] can also be used to predict welding deformation. Compared to TEP-FEM, this method requires significantly less computational time, even for large and complex structures. Furthermore, the elastic FEM only necessitates the elastic modulus and Poisson’s ratio at room temperature, eliminating the need for temperature-dependent material properties. Figure 5 shows the procedures for calculating the final welding-induced deformation of a structure using the inherent strain value, which can be calculated based on the results of maximum temperature, temperature gradient, and reaction force from the heat transfer and TEP analyses.

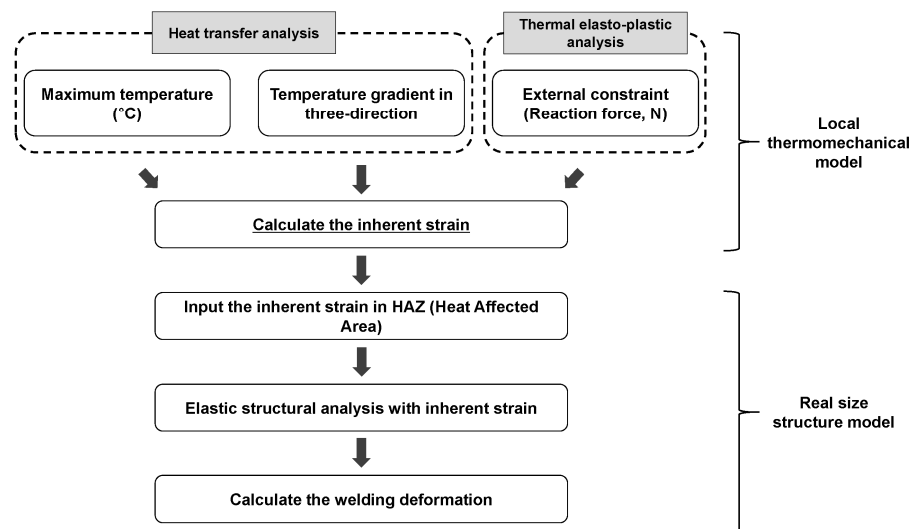


Figure 5. Flow chart of a welding deformation analysis using the inherent strain method [77] (from an open-accessed journal article; permission is not required).

4.4. Heat Source Models

During the arc welding process, a weld pool forms when the base metal reaches its melting point, preparing it for the addition of filler material. Heat source models help

predict the thermal cycle during welding, which is essential for determining the resultant microstructure and mechanical properties of the welded joint. By accurately modeling the heat input, we can optimize welding parameters to reduce defects such as distortion and residual stresses, ensuring the structural reliability of welded aluminum components in marine applications.

The technique used to manipulate the weld pool significantly impacts the quality of the resulting weld bead. One of the earliest analytical approaches to modeling the heat flow during welding involved using conduction heat transfer principles and the Fourier partial differential equation (PDE). To model the weld pool's shape, a moving coordinate system was adopted, allowing for the development of solutions applicable to simple heat sources across various welding scenarios. In the 1960s, the concept of a Gaussian distributed heat source was introduced to approximate the heat flux at the heating spot, as illustrated in Figure 6.

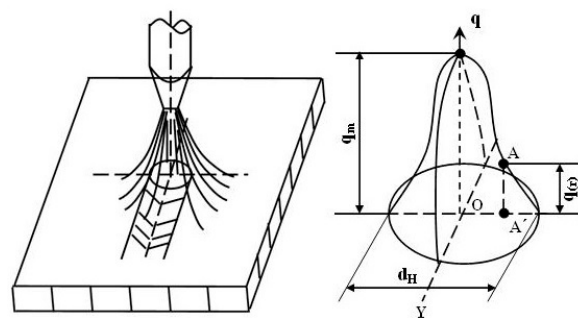


Figure 6. Gaussian distributed heat source model.

The heat flux decreases with distance from the center of the heat source and can be mathematically described as follows:

$$q(r) = q_{max} \exp\left(-\frac{3r^2}{R^2}\right) = \frac{3Q}{\pi R^2} \exp\left(-\frac{3r^2}{R^2}\right) \tag{5}$$

where q_{max} is the maximum heat flux in the center of the heat source, Q is the heat flux of the arc, r is the distance between the point of the heat application and the center of the heat source, and R is the radius of the heating spot.

Later, Goldak et al. [78] suggested that the heat flux within a weld's heat source follows a Gaussian distribution, leading them to propose a semiellipsoidal heat source model. To enhance the model's accuracy, they further introduced a double-ellipsoidal heat source by combining two semiellipsoids with varying parameters, as depicted in Figure 7. This 3D model offers improved predictions of temperature distribution in welded structures, achieving deeper penetration. It also accurately reflects the differing temperature gradients observed at the front and rear parts of the heat source, as verified by experimental data.

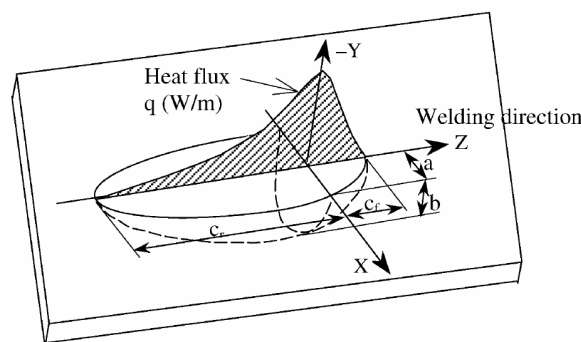


Figure 7. The classic double-ellipsoidal distributed heat source. Adapted from [40], with permission from Springer Nature (Berlin, Germany), 2024.

In this classic model for arc welding, the heat flux distributions within each semiellipsoid are governed by distinct equations:

$$q_f(x, y, z) = \frac{6\sqrt{3}(f_f Q)}{abc_f \pi \sqrt{\pi}} \exp\left(-\frac{3x^2}{a^2} - \frac{3y^2}{b^2} - \frac{3z^2}{c_f^2}\right), z \geq 0$$

$$q_r(x, y, z) = \frac{6\sqrt{3}(f_r Q)}{abc_r \pi \sqrt{\pi}} \exp\left(-\frac{3x^2}{a^2} - \frac{3y^2}{b^2} - \frac{3z^2}{c_r^2}\right), z < 0$$
(6)

where $a, b, c_f,$ and c_r are geometric parameters; f_f and f_r are heat input proportions for the front and rear parts, respectively; Q represents the total input heat energy; and $x, y,$ and z are the coordinates at a given point within the heat source. Note that the welding direction is aligned along the z -axis in these equations. If the welding direction differs, the coordinate system and parameters need to be adjusted accordingly.

It was concluded in [79] that the volumetric heat model (double-ellipsoidal model) demonstrates higher accuracy for simulating the GTAW of aluminum plates compared to the surface heat model. Additionally, using a volumetric heat flux distribution offers a reasonable depiction of residual stress distribution, further validating the appropriateness of the volumetric heat source model for capturing the temperature history during the GTAW process on aluminum plates. Similar conclusions can be found also in research on welded steel structures [80,81]. The boundaries of the FZ and HAZ are sensitive to variations in heat source parameters, making accurate heat source modeling crucial for correctly predicting welding distortion and residual stresses.

In an FSW process, heat production at the contact interfaces between the tool and workpiece is critical to the process. This heat generation can be segmented into three distinct components: (1) heat generated beneath the tool shoulder, (2) heat generated on the pin side of the tool, and (3) heat generated at the tip of the tool pin [82,83], expressed by the following equation:

$$Q_{Total} = Q_1 + Q_2 + Q_3 = \frac{2\pi}{3} \tau_{contact} \omega R_{shoulder}^3 + 2\pi \tau_{contact} \omega R_{probe}^2 H_{probe}$$
(7)

where $R_{shoulder}$ is the tool shoulder radius; R_{probe} and H_{probe} are the radius and height of the tool probe, respectively; ω is the tool angular rotation speed; and $\tau_{contact}$ is contact shear stress.

Figure 8 presents a simplified tool design assumed for analysis, featuring a conical or flat horizontal shoulder surface, a vertical cylindrical probe side surface, and a horizontal flat probe tip surface. The conical shoulder surface is defined by the cone angle α , which is zero in the case of a flat shoulder.

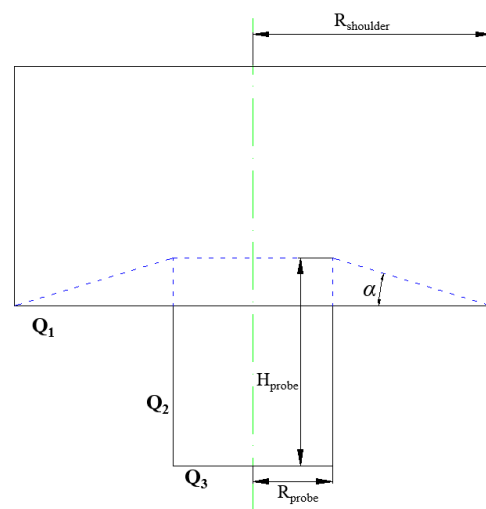


Figure 8. Heat generation contributions in an FSW process [83] (completely redrawn by the authors; permission is not required).

4.5. Computational Resources

Highly detailed FEM simulations, especially those involving complex weld geometries and sophisticated material behavior models, can be computationally intensive. They require significant computational resources and time, which can be a limiting factor in some applications.

In the TEM-FEAs within ANSYS, Solid70 elements, which possess 3D thermal conduction capabilities, are employed for solving the temperature field. When conducting structural analysis, these elements are substituted with equivalent structural elements like Solid185 [41,45,50–53,65]. ANSYS Parametric Design Language (APDL) was utilized to create user-defined macros to simulate the movement of the heating source and the deposition of molten metal droplets on the workpiece [6,17,18]. To accurately simulate the addition of molten weld metal to the workpiece, the element birth and death feature was employed [19,40]. Initially, all weld elements were deactivated at the start of the structural analysis. As the temperature of these elements dropped below the solidification temperature of 610 °C, characteristic of aluminum 6061-T6, they were reactivated [45]. This process effectively models the deposition of weld elements onto the workpiece.

Similar to ANSYS, ABAQUS is also favored by researchers for conducting TEP-FEAs [28,44,47,84,85]. In these simulations, an eight-node linear brick heat transfer element (DC3D8) is utilized for thermal analysis, while the incompatible mode eight-node brick element (C3D8I) is used to simulate the stress–strain fields in mechanical analysis [54]. In addition, an in-house code based on JWRIAN (Joining and Welding Research Institute Analysis, from Osaka University) was developed for analyzing the nonlinear thermomechanical behavior of welded structures in TEP-FEAs [30,48,49,86]. A typical TEP-FEA analysis can take from a few hours to a couple of days on a well-equipped computer.

Additionally, ADINA [87,88], SYSWELD [89–91], Simufact Welding [92], MSC Marc [46], COMSOL Multiphysics [93,94], DEFORM [95,96], and WELDSIM [76] are other popular simulation tools frequently utilized for various welding applications in aluminum alloys. ANSYS and ABAQUS excel in handling complex multiphysics scenarios but might require longer computation time for highly detailed models. On the other hand, SYSWELD specializes in welding and heat treatment simulations and might offer faster solutions for standard welding processes due to its tailored solver and built-in features specific to welding. Apart from the different software used, factors such as model complexity, the solver's parallel processing capabilities, computer configuration, and expertise in advanced user-defined functions or subroutines are key factors that influence computational time.

It is important to note that beyond these traditional methods, the evolving applications of machine learning (ML) [97,98], artificial intelligence (AI) [99,100], digital twin (DT) [101,102], and other emerging technologies in welding simulations highlight the significant potential and promising prospects in this new era. The integration of these new technologies is transforming the field of welding simulations, enhancing the precision, efficiency, and innovative capabilities of welding processes.

Figure 9 displays a digital twin concept for monitoring and control for the lap welding of Al–Cu sheets [101]. Real-time temperature data were utilized to accurately predict the instance of interface melting and control the resulting weld microstructure. The digital twin model was calibrated using a finite element model, which was itself validated through experimental data. A linear-regression-based recursive machine learning model, leveraging a moving average of machine current and temperature history, was employed to predict real-time interface temperatures with high precision. The proposed digital twin model can be used to effectively monitor weld zone temperatures and control the process accordingly. This approach overcomes the impractical measurements associated with using thermocouples and the limitations of infrared sensors in industrial settings, where the interface requiring temperature monitoring is often obscured.

While AI and ML can provide faster solutions in some aspects, their effectiveness heavily depends on the quality and quantity of the data available for training the models.

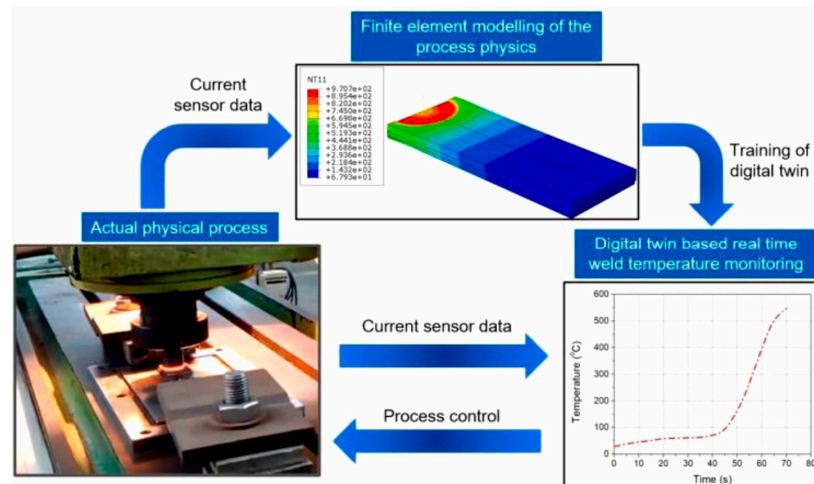


Figure 9. A digital-twin-based monitoring and control system for welding of dissimilar metals. Adapted from [101], with permission from Elsevier, 2024.

4.6. Summary

In this section, the simulation and modeling of welding processes for aluminum alloys are explored extensively through advanced FEM. The focus is on addressing the complexities inherent in welding aluminum, such as rapid heat dissipation, the variation in material properties with temperature, and the effects of welding geometry. Specific attention is given to the accurate modeling of complex joint geometries to ensure high-quality meshes that can accurately capture critical phenomena in the FZ and HAZ. This section also discusses the challenges of modeling the transient material properties of aluminum, which vary significantly under the thermal cycles of welding.

Furthermore, the manuscript delves into the application of uncoupled thermal–mechanical analysis to simulate the welding process, utilizing advanced heat source models to predict temperature distribution more accurately. This sophisticated approach helps in understanding the nonlinear effects of heat input on temperature gradients and residual stresses within welded joints. The comprehensive simulation work discussed in this section not only enhances the understanding of welding-induced phenomena in aluminum structures but also aids in predicting the mechanical behavior of welds, crucial for the design and integrity of marine and offshore structures.

5. Weld-Induced Deformation and Residual Stress: Impact on Structural Integrity

5.1. Measurements of Weld-Induced Deformation and Residual Stress

It is widely acknowledged that the ultimate strength of ship structures is significantly influenced by the shape and amplitude of weld-induced imperfections, as well as the presence of weld-induced residual stress [103,104]. In large-scale fabrication industries, issues such as weld-induced deformation and WRS pose significant challenges by adversely affecting fatigue, fracture resistance, and susceptibility to environmentally assisted cracking (EAC) [6]. An approximate method was suggested to characterize the load-shortening curves of stiffened plates, highlighting the impact of residual stresses [103]. A common practice for aluminum welded stiffened panels [66] revealed that the ultimate limit state (ULS) analysis methods adopted by each industry application provide a high degree of inconsistency. In this respect, the development of the ULS analysis methods common to all types of aluminum welded panel structures is desirable.

Thermocouples, widely used for their broad temperature range, stability, and cost-effectiveness, are popular transducers for measuring temperature in various welding tests [18,40]. Type K thermocouples (chromel/alumel), which support oxidizing atmospheres and have a working range from $-200\text{ }^{\circ}\text{C}$ to $1100\text{ }^{\circ}\text{C}$, were utilized in the welding processes of aluminum alloys [89,96,105]. These thermocouples are commonly welded to

metal parts using a capacitive-discharge technique, as illustrated in Figure 10, to ensure uniformity, or clamped under a screw, with the data collected being transferred to a data logger and a PC for recording.

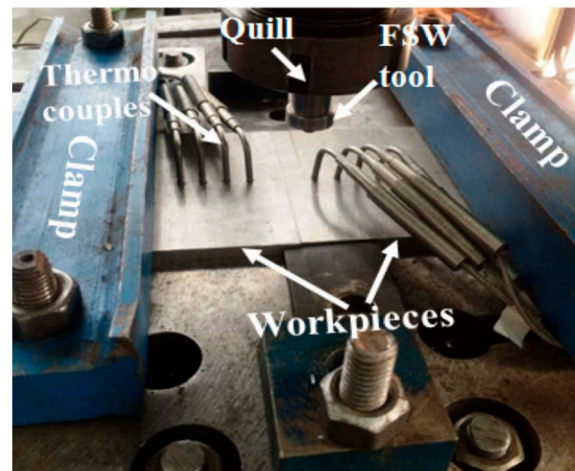


Figure 10. L-shaped K-type thermocouples positioned on an aluminum plate for temperature measurements in an FSW process. Adapted from [106], with permission from Elsevier, 2024.

Figure 10 illustrates the placement of thermocouples on an AA6082 plate considered in an experimental investigation of an FSW process operating at a rotational speed of 500 rpm and a feed rate of 20 mm/s. The dimensions of the plate were 75 mm × 100 mm × 6.35 mm. Eight L-shaped k-type thermocouples, each with a diameter of 3 mm, were positioned at equal distances from the center line to monitor temperature variations—four on the advancing side and four on the retreating side. To secure the thermocouples, 3 mm diameter and 5 mm deep holes were drilled on both sides of the plate. The initial thermocouples on each side were set at 14.5 mm from the center line, located just 3 mm from the end of the shoulder diameter, to protect them from damage during welding. The FSW tool was mounted in the quill of a vertical milling machine and rotated along its longitudinal axis. The two plates were secured to a rigid base plate using clamps to prevent movement during welding. Temperature measurements were taken using a UNILOG instrument equipped with eight channels, consisting of a universal process data recorder that logs the data into an Excel spreadsheet and a channel interface module that relays data from the thermocouples to the recorder.

However, positioning thermocouples accurately within the FZ in arc welding, and in the nugget or areas close to the thermomechanically affected zones (TMAZ) in FSW, presents significant challenges [6]. Thermographic cameras and fiber optic sensors are also employed in various other temperature acquisition systems [105].

Mechanical or optical extensometers are utilized to directly measure strain and deformation on samples during the welding process. Additionally, 3D digital image correlation (DIC) is a noncontact optical method that employs high-speed cameras and software to monitor speckle patterns on the surface of the welding area, enabling the measurement of deformation across the entire field of view. Photogrammetry is another technique that can measure distortion in welded structures [107,108]. Prior to image acquisition, photographs of a calibration grid are taken from various positions and angles to calibrate the camera. Coded targets, as provided by the commercial software PhotoModeler 5, are attached to the plate (see Figure 11), along with other targets that help define the coordinate system. Through the mathematical intersection of straight lines in space, the precise position of each point is determined. Employing photogrammetry, the 3D coordinates of points identified by coded targets are captured, allowing for accurate modeling of deformed surfaces. The photogrammetry technique displayed in the figure was applied in experiments with

small-scaled steel plates, but, undoubtedly, it also holds great potential for application in measuring the deformation in welded aluminum plates.

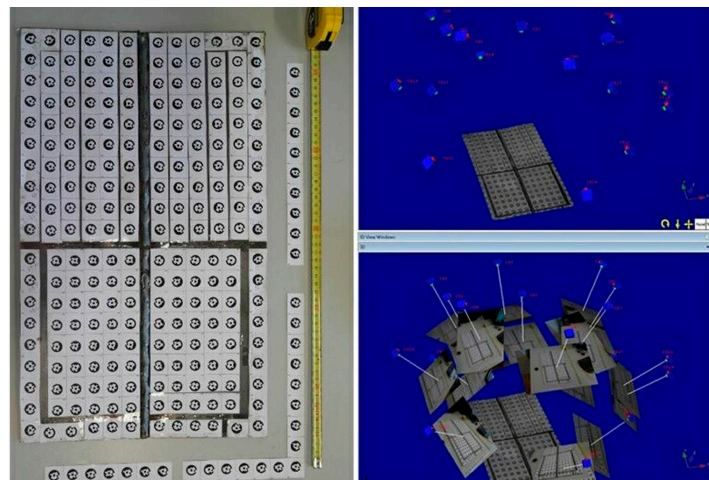


Figure 11. Coded targets attached to a butt-welded plate for photogrammetric modeling. Adapted from [107]; no permission is required from Sage (New York, NY, USA) for Sage authors wishing to reuse their own work.

Essential factors for successful surface measurement include precisely calibrated cameras, images with optimal geometric configuration, adequate local and global image information to identify all matching candidates, and appropriate constraints and strategies for verifying matching results [109]. Laser scanners are also used to generate a high-resolution 3D profile of the workpiece before and after welding, providing a precise assessment of deformation.

The methods being developed to measure residual stress in different components fall into three categories: destructive (including the sectioning method and contour method), semidestructive (such as hole drilling), and nondestructive techniques (including X-ray, neutron diffraction, and ultrasonic inspection). The choice of technique depends on the specific requirements of the measurement and the characteristics of the specimen. Considerations include the depth and penetration of the measurement, the scale (macroscopic or microscopic), the resolution needed, and the composition, geometry, and location of the specimen. X-ray diffraction is a commonly used nondestructive technique for measuring residual stress [73,80,81]. This method determines stresses by measuring the spacing changes in the crystal lattice, considering factors such as Young's modulus, Poisson's ratio, and the elastic anisotropy of the material.

Furthermore, idealizing the distribution of residual stresses has been a typical approach in numerous studies, primarily because obtaining an accurate distribution of WRS in welded structures is challenging [84,104]. The adoption of modern simulation and modeling tools has allowed for better prediction and mitigation of residual stresses during the welding process.

5.2. Effects of Weld-Induced Deformation and Residual Stress and Mitigation Strategies

The most frequent defects in aluminum-plated structures created through welding include initial deflections, residual stresses, and softening in the heat-affected zone (HAZ) [8]. Unlike steel structures, which have extensive data on initial imperfections, information on such imperfections in welded aluminum-plated structures is limited. This scarcity of data introduces greater uncertainty in the design and construction of aluminum vessels compared to their steel counterparts [8].

Research on the elastic local buckling strength of stiffened aluminum plates has shown that ignoring welding residual stresses can reduce buckling strength by about 10–13% with FSW, 14–17% with MIG welding, and 15–18% with TIG welding [110]. Furthermore, a

study [111] examining the ultimate strength of welded aluminum stiffened panels under combined biaxial and lateral loads highlighted the significant role of material softening in the HAZ, while residual stresses were overlooked due to their comparatively minor impact. Nonetheless, all welding effects, including residual stresses, must be carefully considered when analyzing the strength of ship and offshore structures that are (partially) constructed from aluminum alloys.

Methods to mitigate weld-induced distortion and residual stress can be categorized into thermal and mechanical approaches. The thermal method modifies the temperature of the entire component uniformly, either by heating or cooling. For example, circulating water on the underside of plates during welding has been theoretically explored as a way to control distortion [112]. Flame straightening is another thermal technique used for corrective measures post-weld buckling. Additionally, line heating applied on the opposite side of the weld can induce inverse bending, while spot heating can target areas distant from the weld line [86]. The effectiveness of transient thermal tensioning to eliminate buckling distortion in welded assemblies was experimentally demonstrated and verified [113]. On the mechanical side, techniques such as shot peening and laser peening are employed to alleviate undesirable surface tensile stresses and induce beneficial compressive residual stresses [114]. In addition, the factor of time is critical in aluminum welding, both in terms of the welding process itself and the cooling duration that follows. Precise control over the time parameters ensures optimal heat input and distribution, which are crucial for preventing defects such as porosity and excessive distortion. Furthermore, the timing of the cooling phase is essential to achieve the desired mechanical properties and to minimize residual stresses in the weld zone. Effective management of these time-sensitive aspects is integral to maintaining the structural integrity and performance of the welded aluminum components.

The future of mitigating weld-induced deformation and residual stress is promising, with emerging technologies playing a pivotal role. Advances in ML/AI are set to revolutionize how welding parameters are predicted and controlled, potentially allowing real-time adjustments during the welding process to minimize distortions and stresses. Research is also exploring the integration of sensor technology, digital technologies, and intelligent systems within welding setups to provide continuous feedback and adjustments, further enhancing the precision of welding operations [115–117]. This forward-looking approach not only promises to improve the quality and efficiency of welded assemblies but also aims to reduce costs and increase the longevity of engineering structures.

6. Further Discussions

The experimental results outlined in this paper demonstrate how various welding parameters and techniques affect the physical and mechanical properties of aluminum alloys. Notably, they highlight the critical impact of heat input and cooling rates on the formation of residual stresses and deformations. The numerical simulations offered insightful predictions about the thermal and mechanical behavior of welded joints under different conditions. These simulations have been instrumental in understanding the complex interactions within the weld zone, particularly the development of stress concentrations and HAZs. By closely mirroring the experimental conditions, the numerical models not only validated the experimental findings but also provided deeper insights into the variables that are difficult to measure directly, such as internal temperatures and microstructural changes.

The bridge between the experimental and numerical analyses discusses the correlations between observed material responses and predicted outcomes. This integration has proven crucial for refining welding parameters to optimize joint integrity and minimize defects. The discussion also extends to the practical implications of these findings, emphasizing the need for precise control of welding parameters in industrial applications to enhance the durability and reliability of marine structures. Furthermore, the combined insights from these analyses have identified potential areas for future research, particularly in improving simulation accuracy with advanced computational techniques

and exploring new material formulations to enhance weldability and performance under marine conditions.

Throughout the preceding sections, several challenges have been identified in the welding of aluminum alloys for marine applications. These include managing the high thermal conductivity of aluminum, which complicates the welding process due to rapid heat dissipation. This characteristic often leads to inconsistent weld quality, such as porosity and inadequate fusion. Additionally, the susceptibility of aluminum alloys to thermal and residual stresses during welding poses significant challenges in maintaining the structural integrity of the welded joints. The variability in material behavior under different welding settings further complicates the prediction and control of outcomes in real-world applications. These challenges underscore the necessity for advanced research and more refined welding techniques.

Addressing the primary challenges identified in this research, the following points could be considered:

1. Optimize welding parameters:

Develop a comprehensive set of optimized parameters for different aluminum alloys to improve weld consistency and quality. Adjust the heat input to balance between adequate penetration and minimizing residual stress. Implement controlled cooling techniques to manage the thermal gradients that contribute to residual stresses.

2. Enhance material preparation:

Improve surface preparation techniques to reduce contamination and improve the consistency of welds. Standardize cleaning protocols to minimize surface oxides and contaminants before welding. Establish guidelines for handling and storage to preserve surface integrity prior to welding.

3. Advance simulation techniques:

Invest in the development of more sophisticated simulation models that can more accurately predict complex behaviors during welding. Integrate microstructural evolution into simulation models to predict changes in material properties post-welding. Utilize sensors and monitoring technologies to provide real-time feedback on weld quality during the process.

4. Research and development:

Foster continued research into new welding technologies and material formulations that could enhance the weldability and performance of aluminum alloys in marine environments. Explore emerging welding technologies, such as laser welding or hybrid techniques, that could offer more precise control and less thermal distortion. Support the development of new aluminum alloys specifically designed to improve weldability and resistance to environmental factors in marine settings.

5. Enhancing weld monitoring through advanced analytics:

Integrate data derived from NDT methods into AI and ML platforms, allowing predictive models and digital twins to be developed and refined. These models are expected to significantly enhance predictive maintenance, real-time monitoring, and process optimization. In addition, challenges such as ensuring data integrity, managing vast volumes of data, and developing models that can effectively interpret complex data patterns indicative of weld integrity and potential failures are to be addressed.

7. Conclusions and Future Directions

The advancements in aluminum welding for marine structures have provided significant insights into analyzing and minimizing weld-induced deformation and residual stress, crucial for enhancing the structural integrity and performance of marine vessels and platforms. This review has synthesized extensive research spanning experimental

and simulation studies to highlight the critical role of innovative welding techniques in improving the durability and safety of marine infrastructure.

Weld-induced deformations and residual stresses remain a pivotal concern due to their potential to compromise the structural integrity and longevity of welded joints. Emerging welding methods such as FSW and laser welding, compared to the traditional MIG and TIG, have been shown to effectively minimize these defects, offering more reliable and efficient solutions. There is a pressing need to explore advanced simulation technologies and tools that can enable more precise predictions and a better understanding of the complex interactions within the weld zone, facilitating the development of more robust welding strategies. This includes the development of integrated models that combine thermal, mechanical, and metallurgical factors to provide a holistic view of the welding dynamics. Additionally, research should focus on the refinement of additive manufacturing techniques for aluminum, which hold the promise of revolutionizing marine construction with more intricate and lightweight designs.

Validating and calibrating FEM models of aluminum welding requires experimental data, which can sometimes be difficult to obtain. Ensuring that simulation results align with real-world welding behavior demands extensive testing and data collection, which can be costly and time-consuming. More specifically, in the welding simulation by TEP-FEM, significantly high temperatures are induced in the welded structures. The metals have quite different thermal/mechanical behaviors at higher temperatures when compared with their properties at room temperature. Hence, it is essential to take into consideration the temperature-dependent material properties when evaluating weld-induced imperfections. However, there are limited data on the temperature-dependent material properties of the base metal, especially at high temperatures. Addressing these challenges requires a combination of advanced numerical techniques, comprehensive material data, and robust computational resources to ensure that FEM simulations can provide accurate and reliable predictions for aluminum welding processes.

Looking ahead, the field is poised for transformative changes with the integration of digital technologies. The prospective use of machine learning and AI in predictive modeling promises to revolutionize welding practices by enabling real-time control and optimization of welding parameters, thereby reducing defects and improving joint quality. Furthermore, the concept of digital twins could provide a sophisticated means of monitoring and adjusting the welding process in real time, enhancing the adaptability and precision of welding operations in marine construction.

While the marine industry has traditionally lagged behind aerospace and automotive industries in the adoption of new materials technologies, largely due to the stringent safety and durability requirements imposed by the harsh marine environment, it is poised to make significant strides. Ongoing research into new material formulations and advanced welding consumables will continue to support the evolving needs of the marine industry, potentially leading to the development of even more efficient and resilient welding solutions. Continued research and development into new aluminum alloys and their composites will likely yield materials that are not only lighter and stronger but also tailored to withstand the specific challenges of the marine environment. In addition, addressing the environmental impact of welding processes by developing greener and more sustainable practices should also be a priority in future studies.

This review underscores the dynamic nature of the field and sets a clear trajectory for future research and technological advancements, aiming to address the challenges and harness the opportunities that lie ahead in the welding of aluminum structures for marine applications. As we move forward, it will be essential to continue bridging the gap between research and practical applications, ensuring that innovations in welding technology can be effectively translated into improved performance and reliability of marine structures.

Author Contributions: Conceptualization, B.-Q.C.; writing—original draft preparation, B.-Q.C.; writing—review and editing, K.L. and S.X.; visualization, B.-Q.C. All authors have read and agreed to the published version of the manuscript.

Funding: This study contributes to the Strategic Research Plan of the Centre for Marine Technology and Ocean Engineering, which is financed by the Portuguese Foundation for Science and Technology (FCT), under contract UIDB/UIDP/00134/2020.

Data Availability Statement: No new data were created or analyzed in this study. Data sharing is not applicable to this article.

Conflicts of Interest: The authors declare no conflicts of interest.

References

- Magoga, T.; Flockhart, C. Effect of weld-induced imperfections on the ultimate strength of an aluminum patrol boat determined by the ISFEM rapid assessment method. *Ships Offshore Struct.* **2014**, *9*, 218–235. [\[CrossRef\]](#)
- Siengchin, S. A review on lightweight materials for defence applications: Present and future developments. *Def. Technol.* **2023**, *24*, 1–17. [\[CrossRef\]](#)
- Josefson, L.; Anyfantis, K.; Pinheiro, B.D.; Chen, B.Q.; Dong, P.; Ferrari, N.; Gotoh, K.; Huang, J.; Krause, M.; Liu, K.; et al. Committee V. 3: Materials and Fabrication Technology. In Proceedings of the International Ship and Offshore Structures Congress, Vancouver, BC, Canada, 11–15 September 2022; p. D011S001R004. [\[CrossRef\]](#)
- Collette, M. The impact of fusion welds on the ultimate strength of aluminum structures. In Proceedings of the 10th International Symposium on Practical Design of Ships and Other Floating Structures, Houston, TX, USA, October 2007.
- Collette, M. Rapid analysis techniques for ultimate strength predictions of aluminum structures. In *Advances in Marine Structures*; Soares, C.G., Fricke, W., Eds.; Taylor & Francis Group: London, UK, 2011; pp. 109–117.
- Chen, B.Q.; Guedes Soares, C. Numerical investigation on weld-induced imperfections in aluminum ship plates. *J. Offshore Mech. Arct. Eng.* **2019**, *141*, 061605. [\[CrossRef\]](#)
- Wahid, M.A.; Siddiquee, A.N.; Khan, Z.A. Aluminum alloys in marine construction: Characteristics, application, and problems from a fabrication viewpoint. *Mar. Syst. Ocean Technol.* **2020**, *15*, 70–80. [\[CrossRef\]](#)
- Hosseinabadi, O.F.; Khedmati, M.R. A review on ultimate strength of aluminum structural elements and systems for marine applications. *Ocean Eng.* **2021**, *232*, 109153. [\[CrossRef\]](#)
- Georgantzia, E.; Gkantou, M.; Kamaris, G.S. Aluminum alloys as structural material: A review of research. *Eng. Struct.* **2021**, *227*, 111372. [\[CrossRef\]](#)
- Mazzolani, F.M. (Ed.) *Aluminum Structural Design*; Springer: Vienna, Austria, 2003. [\[CrossRef\]](#)
- IACS. W25: *Aluminum Alloys for Hull Construction and Marine Structure, Rev.6*; International Association of Classification Societies: London, UK, 2021.
- Det Norske Veritas. *RU-HSLC: Rules for Classification: High Speed and Light Craft. Part 3 Structures, Equipment, Chapter 9 Direct Calculation Methods*; DNV: Oslo, Norway, 2023.
- Lloyd's Register. *Rules and Regulations for the Classification of Naval Ships*; Lloyd's Register: London, UK, 2023.
- ENV 1999-1.1; Eurocode 9: Design of Aluminum Structures. European Committee for Standardisation: Brussels, Belgium, 2007.
- Vishnukumar, M.; Pramod, R.; Kannan, A.R. Wire arc additive manufacturing for repairing aluminum structures in marine applications. *Mater. Lett.* **2021**, *299*, 130112. [\[CrossRef\]](#)
- Khoshnaw, F.; Krivtsun, I.; Korzhyk, V. Arc welding methods. In *Welding of Metallic Materials*; Elsevier: Amsterdam, The Netherlands, 2023; pp. 37–71. [\[CrossRef\]](#)
- Chen, B.Q.; Guedes Soares, C. Effects of plate configurations on the weld induced deformations and strength of fillet-welded plates. *Mar. Struct.* **2016**, *50*, 243–259. [\[CrossRef\]](#)
- Chen, B.Q.; Guedes Soares, C. Effect of welding sequence on temperature distribution, distortions and residual stress on stiffened plates. *Int. J. Adv. Manuf. Technol.* **2016**, *86*, 3145–3156. [\[CrossRef\]](#)
- Farajkhah, V.; Liu, Y. Effect of fabrication methods on the ultimate strength of aluminum hull girders. *Ocean Eng.* **2016**, *114*, 269–279. [\[CrossRef\]](#)
- Farajkhah, V.; Guedes Soares, C. Finite element study on the ultimate strength of aluminum plates joined by friction stir welding. In *Progress in the Analysis and Design of Marine Structures*; Soares, G., Garbatov, Eds.; Taylor & Francis Group: London, UK, 2017; pp. 609–616. [\[CrossRef\]](#)
- Heidarzadeh, A.; Mironov, S.; Kaibyshev, R.; Çam, G.; Simar, A.; Gerlich, A.; Khodabakhshi, F.; Mostafaei, A.; Field, D.P.; Robson, J.D.; et al. Friction stir welding/processing of metals and alloys: A comprehensive review on microstructural evolution. *Prog. Mater. Sci.* **2021**, *117*, 100752. [\[CrossRef\]](#)
- Meng, X.; Huang, Y.; Cao, J.; Shen, J.; dos Santos, J.F. Recent progress on control strategies for inherent issues in friction stir welding. *Prog. Mater. Sci.* **2021**, *115*, 100706. [\[CrossRef\]](#)
- Singh, V.P.; Patel, S.K.; Ranjan, A.; Kuriachen, B. Recent research progress in solid state friction-stir welding of aluminum–magnesium alloys: A critical review. *J. Mater. Res. Technol.* **2020**, *9*, 6217–6256. [\[CrossRef\]](#)
- Li, S.; Mi, G.; Wang, C. A study on laser beam oscillating welding characteristics for the 5083 aluminum alloy: Morphology, microstructure and mechanical properties. *J. Manuf. Process.* **2020**, *53*, 12–20. [\[CrossRef\]](#)
- Bunaziv, I.; Akselsen, O.M.; Ren, X.; Nyhus, B.; Eriksson, M. Laser beam and laser-arc hybrid welding of aluminum alloys. *Metals* **2021**, *11*, 1150. [\[CrossRef\]](#)

26. Ke, W.; Bu, X.; Oliveira, J.P.; Xu, W.; Wang, Z.; Zeng, Z. Modeling and numerical study of keyhole-induced porosity formation in laser beam oscillating welding of 5A06 aluminum alloy. *Opt. Laser Technol.* **2021**, *133*, 106540. [[CrossRef](#)]
27. Chen, B.Q.; Guedes Soares, C. Study on ultimate strength of ship plates with calculated weld induced residual stress. In *Maritime Technology and Engineering*; Soares, C.G., Santos, T.A., Eds.; Taylor & Francis Group: London, UK, 2015; pp. 513–522. [[CrossRef](#)]
28. Deng, D.; Murakawa, H. Prediction of welding distortion and residual stress in a thin plate butt-welded joint. *Comput. Mater. Sci.* **2008**, *43*, 353–365. [[CrossRef](#)]
29. Wang, D.; Zhang, H.; Gong, B.; Deng, C. Residual stress effects on fatigue behavior of welded T-joint: A finite fracture mechanics approach. *Mater. Des.* **2016**, *91*, 211–217. [[CrossRef](#)]
30. Wang, J.; Yuan, H.; Ma, N.; Murakawa, H. Recent research on welding distortion prediction in thin plate fabrication by means of elastic FE computation. *Mar. Struct.* **2016**, *47*, 42–59. [[CrossRef](#)]
31. Fischer, C.; Fricke, W. Effect of the stress distribution in simple welded specimens and complex components on the crack propagation life. *Int. J. Fatigue* **2016**, *92*, 488–498. [[CrossRef](#)]
32. Rigo, P.; Sarghiuta, R.; Estefen, S.; Lehmann, E.; Otelea, S.C.; Pasqualino, I.; Simonsen, B.C.; Wan, Z.; Yao, T. Sensitivity analysis on ultimate strength of aluminum stiffened panels. *Mar. Struct.* **2003**, *16*, 437–468. [[CrossRef](#)]
33. Yi, H.; Yang, L.; Jia, L.; Huang, Y.; Cao, H. Porosity in wire-arc directed energy deposition of aluminum alloys: Formation mechanisms, influencing factors and inhibition strategies. *Addit. Manuf.* **2024**, *84*, 104108. [[CrossRef](#)]
34. Samiuddin, M.; Li, J.L.; Taimoor, M.; Siddiqui, M.N.; Siddiqui, S.U.; Xiong, J.T. Investigation on the process parameters of TIG-welded aluminum alloy through mechanical and microstructural characterization. *Def. Technol.* **2021**, *17*, 1234–1248. [[CrossRef](#)]
35. Bunaziv, I.; Akselsen, O.M.; Ren, X.; Nyhus, B.; Eriksson, M.; Gulbrandsen-Dahl, S. A review on laser-assisted joining of aluminum alloys to other metals. *Metals* **2021**, *11*, 1680. [[CrossRef](#)]
36. Yang, J.; Oliveira, J.P.; Li, Y.; Tan, C.; Gao, C.; Zhao, Y.; Yu, Z. Laser techniques for dissimilar joining of aluminum alloys to steels: A critical review. *J. Mater. Process. Technol.* **2022**, *301*, 117443. [[CrossRef](#)]
37. Sadeghian, A.; Iqbal, N. A review on dissimilar laser welding of steel-copper, steel-aluminum, aluminum-copper, and steel-nickel for electric vehicle battery manufacturing. *Opt. Laser Technol.* **2022**, *146*, 107595. [[CrossRef](#)]
38. Varshney, D.; Kumar, K. Application and use of different aluminum alloys with respect to workability, strength and welding parameter optimization. *Ain Shams Eng. J.* **2021**, *12*, 1143–1152. [[CrossRef](#)]
39. Masubuchi, K. *Analysis of Welded Structures: Residual Stresses, Distortion, and Their Consequences*; Pergamon Press: Oxford, UK, 1980.
40. Chen, B.Q.; Hashemzadeh, M.; Guedes Soares, C. Numerical and experimental studies on temperature and distortion patterns in butt-welded plates. *Int. J. Adv. Manuf. Technol.* **2014**, *72*, 1121–1131. [[CrossRef](#)]
41. Chen, B.Q.; Guedes Soares, C. Numerical and experimental investigation on the weld induced deformation and residual stress in stiffened plates with brackets. *Int. J. Adv. Manuf. Technol.* **2016**, *86*, 2723–2733. [[CrossRef](#)]
42. Ahmed, S.; Rahman, R.A.U.; Awan, A.; Ahmad, S.; Akram, W.; Amjad, M.; Yahya, M.Y.; Rahimian Kooloor, S.S. Optimization of process parameters in friction stir welding of aluminum 5451 in marine applications. *J. Mar. Sci. Eng.* **2022**, *10*, 1539. [[CrossRef](#)]
43. Bharti, S.; Kumar, S.; Singh, I.; Kumar, D.; Bhurat, S.S.; Abdullah, M.R.; Rahimian Kooloor, S.S. A review of recent developments in friction stir welding for various industrial applications. *J. Mar. Sci. Eng.* **2024**, *12*, 71. [[CrossRef](#)]
44. Zhang, Z.; Zhang, H.W. A fully coupled thermo-mechanical model of friction stir welding. *Int. J. Adv. Manuf. Technol.* **2008**, *37*, 279–293. [[CrossRef](#)]
45. Farajkhah, V.; Liu, Y.; Gannon, L. Finite element study of 3D simulated welding effect in aluminum plates. *Ships Offshore Struct.* **2017**, *12*, 196–208. [[CrossRef](#)]
46. Zhang, Y.; Luo, W.; Zeng, J.; Li, X.; Hu, L.; Deng, D. Preventing crack in an aluminum alloy complex structure during welding process based on numerical simulation technology. *Crystals* **2022**, *12*, 1742. [[CrossRef](#)]
47. Deng, D.; Murakawa, H.; Liang, W. Numerical simulation of welding distortion in large structures. *Comput. Methods Appl. Mech. Eng.* **2007**, *196*, 4613–4627. [[CrossRef](#)]
48. Wang, J.; Shi, X.; Zhou, H.; Yang, Z.; Liu, J. Dimensional precision controlling on out-of-plane welding distortion of major structures in fabrication of ultra large container ship with 20000TEU. *Ocean Eng.* **2020**, *199*, 106993. [[CrossRef](#)]
49. Yi, B.; Wang, J. Mechanism clarification of mitigating welding induced buckling by transient thermal tensioning based on inherent strain theory. *J. Manuf. Process.* **2021**, *68*, 1280–1294. [[CrossRef](#)]
50. Chen, B.Q.; Guedes Soares, C. Experimental and numerical investigation on welding simulation of long stiffened steel plate specimen. *Mar. Struct.* **2021**, *75*, 102824. [[CrossRef](#)]
51. Hashemzadeh, M.; Chen, B.Q.; Guedes Soares, C. Numerical and experimental study on butt weld with dissimilar thickness of thin stainless steel plate. *Int. J. Adv. Manuf. Technol.* **2015**, *78*, 319–330. [[CrossRef](#)]
52. Chen, B.Q.; Guedes Soares, C. A simplified model for the effect of weld induced residual stresses on the longitudinal ultimate strength of stiffened plates. *J. Mar. Sci. Appl.* **2018**, *17*, 57–67. [[CrossRef](#)]
53. Chen, B.Q.; Hashemzadeh, M.; Garbatov, Y.; Guedes Soares, C. Numerical and parametric modeling and analysis of weld induced residual stresses. *Int. J. Mech. Mater. Des.* **2015**, *11*, 439–453. [[CrossRef](#)]
54. Fu, G.; Lourenco, M.I.; Duan, M.; Estefen, S.F. Effect of boundary conditions on residual stress and distortion in T-joint welds. *J. Constr. Steel Res.* **2014**, *102*, 121–135. [[CrossRef](#)]

55. Sánchez, S.J.R.; Martín, F.P.; Melián, A.D. Historical review of the implementation of high-speed vessels in Spain. *J. Marit. Res.* **2022**, *19*, 48–58.
56. Shahraki, J.R.; Davis, M.R.; Shabani, B.; AlaviMehri, J.; Thomas, G.A.; Lavroff, J.; Amin, W.A. Mitigation of slamming of large wave-piercing catamarans. In Proceedings of the 30th Symposium on Naval Hydrodynamics Hobart, Tasmania, Australia, 2–7 November 2014.
57. Caprio, F.; Migali, A.; Pensa, C. Staggered Catamarans: Experimental data and feasibility study for environment friendly service. In Proceedings of the 12th International Congress of the International Maritime Association of the Mediterranean (IMAM 2005), Lisbon, Portugal, 26–30 September 2005; pp. 69–75.
58. da Silva, C.L.M.; Scotti, A. The influence of double pulse on porosity formation in aluminum GMAW. *J. Mater. Process. Technol.* **2006**, *171*, 366–372. [[CrossRef](#)]
59. Liu, Y.; Wang, W.; Xie, J.; Sun, S.; Wang, L.; Qian, Y.; Meng, Y.; Wei, Y. Microstructure and mechanical properties of aluminum 5083 weldments by gas tungsten arc and gas metal arc welding. *Mater. Sci. Eng. A* **2012**, *549*, 7–13. [[CrossRef](#)]
60. Bera, T. The history of development of gas metal arc welding process. *Indian Sci. Cruiser* **2020**, *34*, 64–66. [[CrossRef](#)]
61. Habibi, I.; Triyono; Muhyat, N. A review on aluminum arc welding and its problems. In Proceedings of the 6th International Conference and Exhibition on Sustainable Energy and Advanced Materials (ICE-SEAM 2019), Surakarta, Indonesia, 16–17 October 2019; pp. 819–826. [[CrossRef](#)]
62. Ahmad, R.; Bakar, M.A. Effect of a post-weld heat treatment on the mechanical and microstructure properties of AA6061 joints welded by the gas metal arc welding cold metal transfer method. *Mater. Des.* **2011**, *32*, 5120–5126. [[CrossRef](#)]
63. Mathers, G. *The Welding of Aluminum and Its Alloys*; Woodhead Publishing: Cambridge, UK, 2002.
64. Xu, Y.; Liu, Q.; Xu, J.; Xiao, R.; Chen, S. Review on multi-information acquisition, defect prediction and quality control of aluminum alloy GTAW process. *J. Manuf. Process.* **2023**, *108*, 624–638. [[CrossRef](#)]
65. Lu, Y.; Zhu, S.; Zhao, Z.; Chen, T.; Zeng, J. Numerical simulation of residual stresses in aluminum alloy welded joints. *J. Manuf. Process.* **2020**, *50*, 380–393. [[CrossRef](#)]
66. Paik, J.K.; van der Veen, S.; Duran, A.; Collette, M. Ultimate compressive strength design methods of aluminum welded stiffened panel structures for aerospace, marine and land-based applications: A benchmark study. *Thin-Walled Struct.* **2005**, *43*, 1550–1566. [[CrossRef](#)]
67. Leo, P.; Spigarelli, S.; Cerri, E.; El Mehtedi, M. High temperature mechanical properties of an aluminum alloy containing Zn and Mg. *Mater. Sci. Eng. A* **2012**, *550*, 206–213. [[CrossRef](#)]
68. Kumar, P.V.; Reddy, G.M.; Rao, K.S. Microstructure, mechanical and corrosion behavior of high strength AA7075 aluminum alloy friction stir welds—Effect of post weld heat treatment. *Def. Technol.* **2015**, *11*, 362–369. [[CrossRef](#)]
69. Temmar, M.; Hadji, M.; Sahraoui, T. Effect of post-weld aging treatment on mechanical properties of Tungsten Inert Gas welded low thickness 7075 aluminum alloy joints. *Mater. Des.* **2011**, *32*, 3532–3536. [[CrossRef](#)]
70. Thornton, M.; Han, L.; Shergold, M. Progress in NDT of resistance spot welding of aluminum using ultrasonic C-scan. *Ndt E Int.* **2012**, *48*, 30–38. [[CrossRef](#)]
71. Passini, A.; Oliveira, A.C.D.; Riva, R.; Travessa, D.N.; Cardoso, K.R. Ultrasonic inspection of AA6013 laser welded joints. *Mater. Res.* **2011**, *14*, 417–422. [[CrossRef](#)]
72. Azeez, S.T.; Mashinini, P.M. Radiography examination of friction stir welds of dissimilar aluminum alloys. *Mater. Today Proc.* **2022**, *62*, 3070–3075. [[CrossRef](#)]
73. Galos, J.; Ghaffari, B.; Hetrick, E.T.; Jones, M.H.; Benoit, M.J.; Wood, T.; Sanders, P.G.; Easton, M.A.; Mouritz, A.P. Novel non-destructive technique for detecting the weld fusion zone using a filler wire of high x-ray contrast. *NDT E Int.* **2021**, *124*, 102537. [[CrossRef](#)]
74. Reddy, K.A. Non-destructive testing, evaluation of stainless steel materials. *Mater. Today Proc.* **2017**, *4*, 7302–7312. [[CrossRef](#)]
75. Deivanai, S.; Soni, M. Non destructive testing and analysis of friction stir welded aluminum alloy 2024 pipes. *Mater. Today Proc.* **2022**, *56*, 3721–3726. [[CrossRef](#)]
76. Zhu, X.K.; Chao, Y.J. Effects of temperature-dependent material properties on welding simulation. *Comput. Struct.* **2002**, *80*, 967–976. [[CrossRef](#)]
77. Kang, S.; Kim, J.; Jang, Y.; Lee, K. Welding deformation analysis, using an inherent strain method for friction stir welded electric vehicle aluminum battery housing, considering productivity. *Appl. Sci.* **2019**, *9*, 3848. [[CrossRef](#)]
78. Goldak, J.A.; Chakravarti, A.; Bibby, M.J. A new finite element model for welding heat source. *Metall. Trans. B* **1984**, *15B*, 299–305. [[CrossRef](#)]
79. Dehkordi, Y.G.; Anaraki, A.P.; Shahani, A.R. Investigation of heat source models and process factors on temperature and residual stress in GTAW of aluminum plates. *Russ. J. Non-Ferr. Met.* **2019**, *60*, 450–462. [[CrossRef](#)]
80. Hashemzadeh, M.; Chen, B.Q.; Guedes Soares, C. Evaluation of multi-pass welding-induced residual stress using numerical and experimental approaches. *Ships Offshore Struct.* **2018**, *13*, 847–856. [[CrossRef](#)]
81. Chen, B.Q.; Hashemzadeh, M.; Guedes Soares, C. Validation of numerical simulations with X-ray diffraction measurements of residual stress in butt-welded steel plates. *Ships Offshore Struct.* **2018**, *13*, 273–282. [[CrossRef](#)]
82. Akbari, M.; Asadi, P.; Sadowski, T. A Review on Friction Stir Welding/Processing: Numerical Modeling. *Materials* **2023**, *16*, 5890. [[CrossRef](#)]

83. Schmidt, H.; Hattel, J.; Wert, J. An analytical model for the heat generation in friction stir welding. *Model. Simul. Mater. Sci. Eng.* **2004**, *12*, 143–157. [[CrossRef](#)]
84. Khan, I.; Zhang, S. Effects of welding induced residual stress on ultimate strength of plates and stiffened panels. *Ships Offshore Struct.* **2011**, *6*, 297–309. [[CrossRef](#)]
85. Cooper, D.R.; Allwood, J.M. The influence of deformation conditions in solid-state aluminum welding processes on the resulting weld strength. *J. Mater. Process. Technol.* **2014**, *214*, 2576–2592. [[CrossRef](#)]
86. Ma, N.S.; Wang, J.C.; Okumoto, Y. Out-of-plane welding distortion prediction and mitigation in stiffened welded structures. *Int. J. Adv. Manuf. Technol.* **2016**, *84*, 1371–1389. [[CrossRef](#)]
87. Lacki, P.; Derlatka, A. Experimental and numerical investigation of aluminum lap joints made by RFSSW. *Meccanica* **2016**, *51*, 455–462. [[CrossRef](#)]
88. Mochizuki, M. Control of welding residual stress for ensuring integrity against fatigue and stress–corrosion cracking. *Nucl. Eng. Des.* **2007**, *237*, 107–123. [[CrossRef](#)]
89. Tsirkas, S.A. Numerical simulation of the laser welding process for the prediction of temperature distribution on welded aluminum aircraft components. *Opt. Laser Technol.* **2018**, *100*, 45–56. [[CrossRef](#)]
90. Lima, T.R.; Tavares, S.M.; De Castro, P.M. Residual stress field and distortions resulting from welding processes: Numerical modelling using Sysweld. *Ciência Tecnol. Dos Mater.* **2017**, *29*, e56–e61. [[CrossRef](#)]
91. Arhumah, Z.; Pham, X.-T. Microstructure and Thermal Mechanical Behavior of Arc-Welded Aluminum Alloy 6061-T6. *J. Manuf. Mater. Process.* **2024**, *8*, 110. [[CrossRef](#)]
92. Su, C.; Zhou, J.Z.; Ye, Y.X.; Huang, S.; Meng, X.K. Study on fiber laser welding of AA6061-T6 samples through numerical simulation and experiments. *Procedia Eng.* **2017**, *174*, 732–739. [[CrossRef](#)]
93. Bachmann, M.; Avilov, V.; Gumenyuk, A.; Rethmeier, M. About the influence of a steady magnetic field on weld pool dynamics in partial penetration high power laser beam welding of thick aluminum parts. *Int. J. Heat Mass Transf.* **2013**, *60*, 309–321. [[CrossRef](#)]
94. Pandian, V.; Kannan, S. Numerical prediction and experimental investigation of aerospace-grade dissimilar aluminum alloy by friction stir welding. *J. Manuf. Process.* **2020**, *54*, 99–108. [[CrossRef](#)]
95. Sibalic, N.; Vukcevic, M. Numerical Simulation for FSW Process at Welding Aluminum Alloy AA6082-T6. *Metals* **2019**, *9*, 747. [[CrossRef](#)]
96. Rao, J.C.; Harikiran, V.; Gurudatta, K.S.S.; Raju, M.K. Temperature and strain distribution during friction stir welding of AA6061 and AA5052 aluminum alloy using deform 3D. *Mater. Today: Proc.* **2022**, *59*, 576–582. [[CrossRef](#)]
97. Verma, S.; Misra, J.P.; Popli, D. Modeling of friction stir welding of aviation grade aluminum alloy using machine learning approaches. *Int. J. Model. Simul.* **2022**, *42*, 1–8. [[CrossRef](#)]
98. Mongan, P.G.; Hinchey, E.P.; O’Dowd, N.P.; McCarthy, C.T. Quality prediction of ultrasonically welded joints using a hybrid machine learning model. *J. Manuf. Process.* **2021**, *71*, 571–579. [[CrossRef](#)]
99. Cardellicchio, A.; Nitti, M.; Patruno, C.; Mosca, N.; di Summa, M.; Stella, E.; Renò, V. Automatic quality control of aluminum parts welds based on 3D data and artificial intelligence. *J. Intell. Manuf.* **2024**, *35*, 1629–1648. [[CrossRef](#)]
100. Gupta, S.K.; Pandey, K.N.; Kumar, R. Artificial intelligence-based modelling and multi-objective optimization of friction stir welding of dissimilar AA5083-O and AA6063-T6 aluminum alloys. *Proc. Inst. Mech. Eng. Part L J. Mater. Des. Appl.* **2018**, *232*, 333–342. [[CrossRef](#)]
101. Maity, D.; Premchand, R.; Muralidhar, M.; Racherla, V. Real-time temperature monitoring of weld interface using a digital twin approach. *Measurement* **2023**, *219*, 113278. [[CrossRef](#)]
102. Chen, G.; Zhu, J.; Zhao, Y.; Hao, Y.; Yang, C.; Shi, Q. Digital twin modeling for temperature field during friction stir welding. *J. Manuf. Process.* **2021**, *64*, 898–906. [[CrossRef](#)]
103. Gordo, J.M.; Guedes Soares, C. Approximate method to evaluate the hull girder collapse strength. *Mar. Struct.* **1996**, *9*, 449–470. [[CrossRef](#)]
104. Paik, J.K.; Sohn, J.M. Effects of welding residual stresses on high tensile plate ultimate strength: Nonlinear finite element method investigations. *J. Offshore Mech. Arct. Eng.* **2012**, *134*, 021401. [[CrossRef](#)]
105. Moreira, P.M.; Frazao, O.; Tavares, S.M.; de Figueiredo, M.A.; Restivo, M.T.; Santos, J.L.; de Castro, P.M. Temperature field acquisition during gas metal arc welding using thermocouples, thermography and fibre Bragg grating sensors. *Meas. Sci. Technol.* **2007**, *18*, 877–883. [[CrossRef](#)]
106. Verma, S.; Misra, J.P. Study on temperature distribution during Friction Stir Welding of 6082 aluminum alloy. *Mater. Today Proc.* **2017**, *4*, 1350–1356. [[CrossRef](#)]
107. Chen, B.Q.; Garbatov, Y.; Guedes Soares, C. Measurement of weld induced deformations in three-dimensional structures based on photogrammetry technique. *J. Ship Prod. Des.* **2011**, *27*, 51–62.
108. Chen, B.Q.; Guedes Soares, C. Deformation measurements in welded plates based on close-range photogrammetry. *Proc. Inst. Mech. Eng. Part B J. Eng. Manuf.* **2016**, *230*, 662–674. [[CrossRef](#)]
109. Romero, E.; Chapuis, J.; Bordreuil, C.; Soulié, F.; Fras, G. Image processing and geometrical analysis for profile detection during pulsed gas metal arc welding. *Proc. IMechE Part B J. Eng. Manuf.* **2013**, *227*, 396–406. [[CrossRef](#)]
110. Mohammadi, M.; Khedmati, M.R.; Bahmyari, E. Elastic local buckling strength analysis of stiffened aluminium plates with an emphasis on the initial deflections and welding residual stresses. *Ships Offshore Struct.* **2019**, *14*, 125–140. [[CrossRef](#)]

111. Wang, X.; Yu, Z.; Amdahl, J. Ultimate strength of welded aluminum stiffened panels under combined biaxial and lateral loads: A numerical investigation. *Mar. Struct.* **2024**, *97*, 103654. [[CrossRef](#)]
112. Adak, M.; Mandal, N.R. Numerical and experimental study of mitigation of welding distortion. *Appl. Math. Model.* **2010**, *34*, 146–158. [[CrossRef](#)]
113. Deo, M.V.; Michaleris, P. Mitigation of welding induced buckling distortion using transient thermal tensioning. *Sci. Technol. Weld. Join.* **2003**, *8*, 49–54. [[CrossRef](#)]
114. Zondi, M.C. Factors that affect welding-induced residual stress and distortions in pressure vessel steels and their mitigation techniques: A review. *J. Press. Vessel Technol.* **2014**, *136*, 040801. [[CrossRef](#)]
115. Guo, Q.; Yang, Z.; Xu, J.; Jiang, Y.; Wang, W.; Liu, Z.; Zhao, W.; Sun, Y. Progress, challenges and trends on vision sensing technologies in automatic/intelligent robotic welding: State-of-the-art review. *Robot. Comput.-Integr. Manuf.* **2024**, *89*, 102767. [[CrossRef](#)]
116. Kumar, S.; Sharma, K.; Mishra, V.; Maan, V. A structural model of Welding 4.0 implementation challenges. *Int. J. Interact. Des. Manuf.* **2024**, *18*, 1243–1254. [[CrossRef](#)]
117. Xu, J.; Liu, Q.; Xu, Y.; Xiao, R.; Hou, Z.; Chen, S. Review on the Application of the Attention Mechanism in Sensing Information Processing for Dynamic Welding Processes. *J. Manuf. Mater. Process.* **2024**, *8*, 22. [[CrossRef](#)]

Disclaimer/Publisher's Note: The statements, opinions and data contained in all publications are solely those of the individual author(s) and contributor(s) and not of MDPI and/or the editor(s). MDPI and/or the editor(s) disclaim responsibility for any injury to people or property resulting from any ideas, methods, instructions or products referred to in the content.